Nature Environment and Pollution Technology
An International Quarterly Peer-Reviewed Open Access Journal

p-ISSN: 0972-6268 | e-ISSN: 2395-3454 Vol. 25 | No. 4 | Article ID D1894 | 2026

RESEARCH ARTICLE https://doi.org/10.46488/NEPT.2026.v25i04.D1894 OPEN ACCESS

Dispersion Modeling of SO_2 and NO_2 Emissions Using AERMOD on Ambient Air Quality at Steam Power Plant PT.X in Southeast Sulawesi, Indonesia

Nur Miftahuljannah, Sumarni Hamid Aly† and Muralia Hustim
Department of Environmental Engineering, Hasanuddin University, Malino Str. km 6, Gowa, South Sulawesi, 92171, Indonesia
†Corresponding author: Sumarni Hamid Aly; marni_hamidaly@yahoo.com

ARTICLE HISTORY

Received: 24-02-2026
Revised: 26-02-2026
Accepted: 16-03-2026

KEYWORDS

AERMOD
Dispersion modeling
Model validation
Steam power plant industry
SO_2 and NO_2 emissions
Ambient air quality

CITE THIS ARTICLE

Miftahuljannah, N., Aly, S.H. and Hustim, M., 2026. Dispersion modeling of SO_2 and NO_2 emissions using AERMOD on ambient air quality at steam power plant PT.X in southeast Sulawesi, Indonesia. *Nature Environment and Pollution Technology*, 25(4), D1894. https://doi.org/10.46488/NEPT.2026.v25i04.D1894

COPYRIGHT & LICENCE

© 2026 The Authors
Open Access under CC BY 4.0.

PUBLISHED BY

TECHNOSCIENCE PUBLICATIONS

ABSTRACT

This study aims to analyze SO_2 and NO_2 concentrations around the PT.X power plant through direct measurements, model their distribution patterns using AERMOD, and evaluate the model's performance using RMSE, MBE, and R statistical tests. Monitoring was conducted at two monitoring points (PLTU PT.X Area and Nii Tanasa Village) over four 1-hour intervals (morning, afternoon, evening, night) using an Impinger Air Sampler. The results show that the highest field-measured SO_2 (39.95 μg m^{-3}) and NO_2 (14.82 μg m^{-3}) occurred during the afternoon, whereas AERMOD predicted peak concentrations at night, reaching SO_2 (31.87 μg m^{-3}) and NO_2 (10.56 μg m^{-3}) at the PLTU PT.X monitoring point, indicating stable atmospheric conditions. Pollutant distribution aligns with the prevailing north-northeast winds, with concentrations decreasing with distance and remaining within regulatory limits. Statistical validation for SO_2 and NO_2 yielded RMSE values of 14 μg m^{-3} and 5.37 μg m^{-3}, MBE of -10.44 μg m^{-3} and -4.32 μg m^{-3}, and R of 0.36 and 0.12, respectively. These values reflect the inherent challenges of aligning short-term field data with long-term dispersion modeling. It is concluded that spatial proximity to emission sources is the primary factor determining concentration patterns. While acknowledging temporal limitations for full-scale validation, the AERMOD model serves as a valuable preliminary screening tool for these distribution patterns. These findings provide an initial overview to inform decision-making and support the development of effective emission mitigation and environmental management strategies for the surrounding areas.

1. INTRODUCTION

Steam Power Plants (PLTU) serve as a vital energy source for industrial activities (Munawaroh et al. 2019). The primary fuel utilized in the power plant industry is coal (Oktaviani et al. 2023). This reliance stems from the abundant supply of coal, which is utilized as a major electricity source for various industries, particularly steam power generation (Rahmadina 2022).

PLTU PT.X, located in Lalonggasumeeto District, Konawe Regency, Southeast Sulawesi, was established in 2007 and has been in commercial operation since 2013, utilizing low-calorie lignite coal for power generation (Barata 2024). In its operations, PLTU PT.X, which also utilizes coal, has the potential to emit gaseous pollutants such as Sulfur Dioxide (SO_2) and Nitrogen Dioxide (NO_2). It is critical to monitor these emissions as they disperse into the surrounding air and pose potential risks to local public health (Ningsih 2020). SO_2 exposure can lead to respiratory tract irritation and decreased pulmonary function (Tampa et al. 2020); similarly, NO_2 can cause mucous membrane irritation and potentially lead to pulmonary

edema in cases of high-dose, long-term exposure, acting as a primary trigger for respiratory diseases (Alchamdani 2019). This health risk is evidenced by the increase in cases of acute respiratory infection reported at the Lalonggasumeeto Public Health Center from 2015 to 2020 (Halulanga et al. 2021).

In anticipating the potential negative impacts of PLTU PT.X activities, gas-emission dispersion modeling is needed as an initial mitigation step to analyze air quality relative to pollutant distribution, establish relationships between emitted pollutants and their concentrations, and identify affected areas (Wangsa et al. 2022). Various models commonly used in predicting air pollutant dispersion include HYSPLIT, CALINE-4, AERMOD, CALPUFF, WRF-Chem, and GRAL (Alviani et al. 2022). This study uses AERMOD to model emission dispersion. This model is recommended by the United States Environmental Protection Agency (US EPA) because it has been proven effective in analyzing, predicting, and simulating the distribution of SO_2 and NO_2 emissions (Zakaria et al. 2020), taking into account meteorological and topographic factors (Putra & Nisa 2023), and can estimate the air quality impact of up to 50 different sources, whose configurations include points, areas, and volumes (Nugraha et al. 2023). Widely recognized as a leading Gaussian plume model, AERMOD is utilized to estimate the environmental consequences resulting from multiple air pollution sources (Salari et al. 2026). This method has also been widely applied internationally to predict pollutant concentrations from various industrial point sources. For example, a study in Cam Pha, Vietnam, showed that AERMOD was successfully applied to evaluate the impact of power plant emissions, involving model validation with observational data (Tran et al. 2022). Similarly, in Indonesia, AERMOD has been used to predict SO_2 and NO_2 dispersion at the PLTU PT. Semen Tonasa using instantaneous measurements and modeling, but validation of the results has not been consistently carried out using robust statistical metrics (Junarto 2021). Previous research (Halulanga et al. 2021) was also conducted at the PLTU PT.X Kendari, but it was limited to direct measurements without using air dispersion modeling or comparing the results of both.

While previous studies have employed the AERMOD model to simulate pollutant dispersion in various industrial contexts, a significant research gap remains regarding the lack of statistical validation using local ambient data, particularly in Southeast Sulawesi. Most existing studies in similar regions focus solely on simulation results without comparing them to direct field measurements through rigorous statistical testing. The novelty of this research lies in its integrated approach that performs a preliminary performance evaluation using local ambient air data collected directly from the PLTU PT.X vicinity by applying multi-parameter statistical indicators, including Root Mean Square Error (RMSE), Mean Bias Error (MBE), and Correlation Coefficient (R). This study seeks to assess the level of agreement between

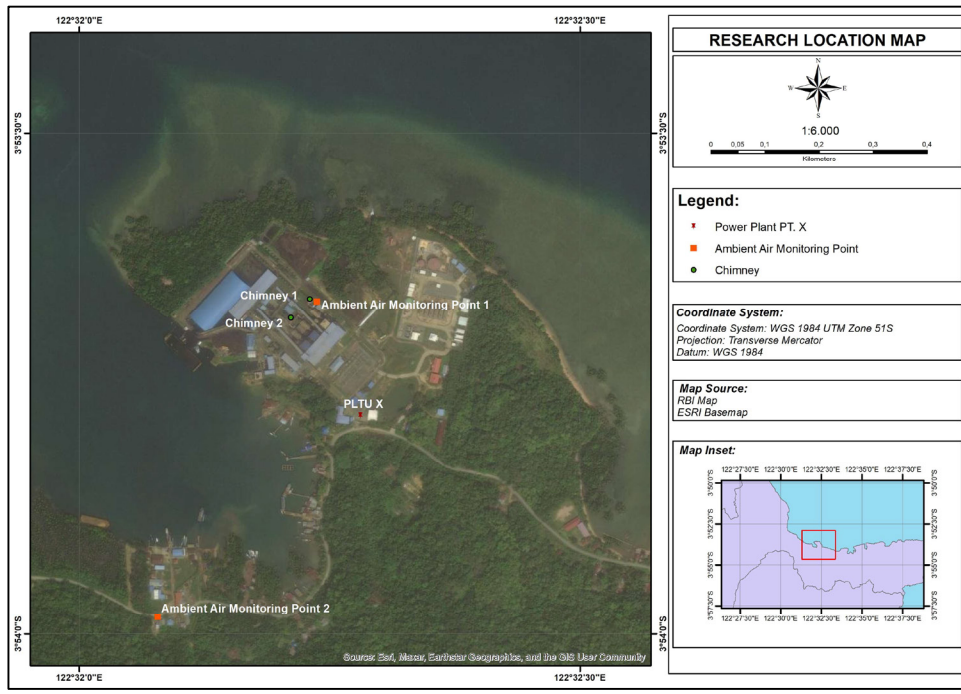


Fig. 1: Research location map.

the model and short-term field observations. Furthermore, this study provides an initial dispersion profile for PLTU PT.X, addressing the absence of prior research at this specific power plant. Therefore, this study aims to analyze SO_2 and NO_2 concentrations around the PLTU PT.X through direct measurements, model their dispersion patterns using AERMOD, and evaluate the model's performance during representative operational periods, while acknowledging the temporal constraints of the field data.

2. MATERIALS AND METHODS

2.1. Study Area

This study was conducted around the PLTU PT.X in Lalonggasumeeto Subdistrict, Konawe Regency, Southeast Sulawesi, Indonesia, with two ambient air monitoring points (Point 1 in the area of PLTU PT.X and Point 2 in Nii Tanasa Village). The location of monitoring points was determined in accordance with SNI 19-7119.6-2005 to ensure representation of the potential impact zone from the pollutant. The selection of these two points was strategically based on the prevailing wind direction and the proximity to sensitive receptors; Point 1 represents the immediate source-proximity monitoring location within the industrial footprint to evaluate near-field dispersion behavior, while Point 2 represents the nearest residential area located downwind. This placement ensures that even with a limited number of points, the study captures the most critical spatial variability of pollutant impact on both the industrial site and the surrounding community. The research location map is shown in Fig. 1.

2.2. Data Collection

Data collection consists of primary and secondary data. Primary data include direct measurements of SO_2 and NO_2 concentrations at two specified points, which are then evaluated against the Indonesian Ambient Air Quality Standards (Government Regulation Number 22 of 2021). Secondary data include meteorological data and chimney specifications of PLTU PT.X and topographic maps, which serve as important input data for dispersion modeling using AERMOD software. The model's performance was evaluated by comparing AERMOD predictions with direct measurement data corresponding to the specific sampling periods using Root Mean Square Error (RMSE), Mean Bias Error (MBE), and Correlation Coefficient (R).

2.2.1. Ambient Air Sampling

Ambient air sampling for SO_2 and NO_2 was carried out using an Impinger Air Sampler, as shown in Fig. 2.

Field measurements were conducted on October 21, 2024, which represents the transition period between the dry and rainy seasons in Southeast Sulawesi. To capture diurnal atmospheric variations, sampling was performed at four specific time intervals: morning (07:00–08:00 WITA), afternoon (13:00–14:00 WITA), evening (16:00–17:00 WITA), and night (19:00–20:00 WITA). These discrete measurements were utilized as preliminary diurnal representative spot samples to evaluate the level of agreement between field observations and the AERMOD model's hourly performance. While this one-day sampling does not constitute a continuous 24-hour integrated average, the sampling intervals were conducted in accordance with the 1-hour ambient air sampling principles and standards outlined in Indonesian Government Regulation No. 22 of 2021. To account for long-term variability, the AERMOD simulation itself utilized a comprehensive one-year hourly meteorological dataset for 2024. This approach allows for a comparison between predicted and observed concentrations during specific atmospheric windows, although it is



Fig. 2: Impinger air sampler.

acknowledged that a more extensive monitoring dataset would be required for a full-scale seasonal or annual model validation.

2.2.2. Meteorological Data

Meteorological data for 2024 were obtained from the Copernicus Climate Change Service (C3S) Climate Data Store, specifically utilizing the ERA5 hourly reanalysis dataset on single levels. Parameters extracted included surface thermal radiation, cloud cover, 2-m temperature, relative humidity, surface pressure, 10-m wind direction, 10-m wind speed, ceiling height, and total precipitation. The data were extracted for the grid corresponding to the study area and synchronized with the surface characteristics of the Kendari Maritime Meteorological Station (BMKG). Station metadata and surface parameters (albedo, Bowen ratio, and surface roughness) were assigned based on local conditions. The raw Copernicus dataset was preprocessed and formatted using the AERMET processor (along with WRPLOT for wind rose visualization) to construct the required surface (.sfc) and profile (.pfl) input files for AERMOD dispersion simulations. Details of the meteorological station information are listed in Table 1.

Table 1: Meteorological station information.

Information Type	Description
Station Name	Kendari Maritime Meteorological Station
Station ID	97144
Latitude	03° 58’ 12.360” S
Longitude	122° 35’ 22.200” E
City	Kendari
Country	Indonesia
Station Elevation	2 m
Time Zone	WITA (UTC +8)

2.2.3. PLTU PT.X Chimney Specifications

The technical specifications of the chimneys, including height, diameter, gas exit velocity, and temperature, were obtained from the PLTU PT.X operational reports for February 2024, as presented in Table 2. These values represent the plant’s typical baseline operating conditions at steady-state load, which remained stable and representative of normal operations during the October 21, 2024 field monitoring period. These physical parameters are essential for determining the plume rise and initial dispersion behavior in the AERMOD model. To ensure the accuracy of the emission input, the emission rates (g s^{-1}) were calculated using the U.S. EPA emission factor method based on fuel consumption, while the measured stack concentrations from the Analysis Report were utilized to verify and ensure that the calculated rates were consistent with the actual monitored conditions.

2.3. Data Analysis

Data analysis was performed using measured ambient air concentration data and secondary input data (meteorological and emission data). The analysis procedures performed in this study included:

2.3.1. Processing Meteorological Data with WRPLOT

WRPLOT was used to process meteorological data into wind rose maps, which visually depict the direction and speed of prevailing winds during the study period. The results are saved in SAMSON (.SAM) format for use as input to the AERMET processor. The stages of data processing in WRPLOT are shown in Fig. 3.

The generated wind rose map was used as meteorological input data for dispersion model simulations in AERMOD. The dominant wind direction and speed patterns greatly determine the potential spread of pollutants. The 2024 wind rose map is presented in Fig. 4.

Table 2: Chimney physical specifications of PLTU PT.X.

No.	Parameters	Chimney 1	Chimney 2
1	Chimney Coordinate (UTM) X	448618.00	448585.00
	Chimney Coordinate (UTM) Y	9569519.00	9569480.00
2	Fuel Type	Lignite Coal	Lignite Coal
3	Chimney Height (m)	45	45
4	Chimney Diameter (m)	2.2	2.2
5	Gas Temperature (°C)	129	130
6	Gas Exit Velocity (m s^{-1})	4.72	4.83
7	Emission Flow Rate (m^3 s^{-1})	17.9	18.31
8	Fuel Consumption (tons/month)	9000	9000
9	Elevation (m)	10	10

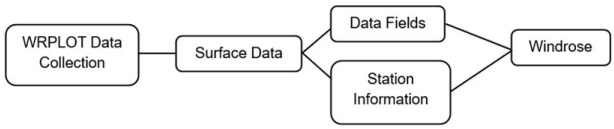


Fig. 3: WRPLOT data processing stages.

Based on Fig. 4(a) and 4(b), the results of the 2024 wind rose analysis show that the dominant direction for the highest wind speed (>9.00 m s^{-1}) is north, with a frequency of 22.8%. The most frequent wind class is the low speed range (0.00–3.00 m s^{-1}), which blows mainly from the west and contributes the highest frequency of 41.9%. This dominant wind pattern is crucial for understanding the potential spread of pollutants originating from the steam power plant.

2.3.2. Calculation of Emission Rate

To meet the input requirements of the AERMOD dispersion model, the emission rates were determined in grams per second (g s^{-1}). The calculation of the flue gas emission rate was carried out to estimate the stack emissions based on February 2024 operational data and to calculate the emission values for October 2024 using the United States Environmental Protection Agency (US EPA 2024) emission factor method (Equation 1). Instead of relying solely on concentration-to-mass conversion, this study utilized an activity-based approach where monthly fuel consumption data were converted into a continuous mass flow rate (tons/second). This ensures that the resulting emission values reflect the plant's actual operational load during the study period. The calculation results, incorporating the efficiency of the emission control systems, are listed in Table 3.

$$E = A \times EF \times [1 - (ER/100)] \quad \ldots(1)$$

Where: E – gas emission rate (g s^{-1}), A – amount of fuel burned (converted from tons/month to tons/second), EF – emission factor (lb/ton or g/ton), ER – emission control efficiency (if there is a scrubber or other system) (e.g. 0.90 for 90%).

The mass emission rates (E) used as AERMOD inputs were derived through a clear, step-by-step application of the activity-based approach. First, the monthly fuel consumption of 9000 tons was converted into a continuous mass flow rate (A) by dividing it by the total seconds in a 30-day month, resulting in 0.00347 tons/second. This value was then applied to Equation 1 using the U.S. EPA AP-42 emission factors (EF) of 15.15 kg/ton for SO_2 and 3.86 kg/ton for NO_x (expressed as NO_2), while incorporating the efficiency of the emission control systems (ER) of 90% and 85%, respectively. This calculation process yielded final emission rates of 5.26 g s^{-1} for SO_2 and 2.01 g s^{-1} for No_x (as NO_2) per chimney. For dispersion modeling in AERMOD, a conservative 100% conversion assumption was applied for NO_2 to evaluate maximum potential impact. These derived rates serve as the definitive source-term inputs for the dispersion model,

Table 3: Emission rate calculation results.

Parameters	SO_2		NO_2	
Emission Factor (lb/ton)	33.4		8.5	
Emission Factor (kg/ton)	15.15		3.86	
Fuel Consumption (tons/month)	9000		9000	
Fuel Consumption (tons/second)	0.00347		0.00347	
Emission Control Efficiency (%)	90		85	
Emission Rate (g s^{-1})	C1	C2	C1	C2
	5.26	5.26	2.01	2.01

Notes: C1 (chimney 1); C2 (chimney 2)

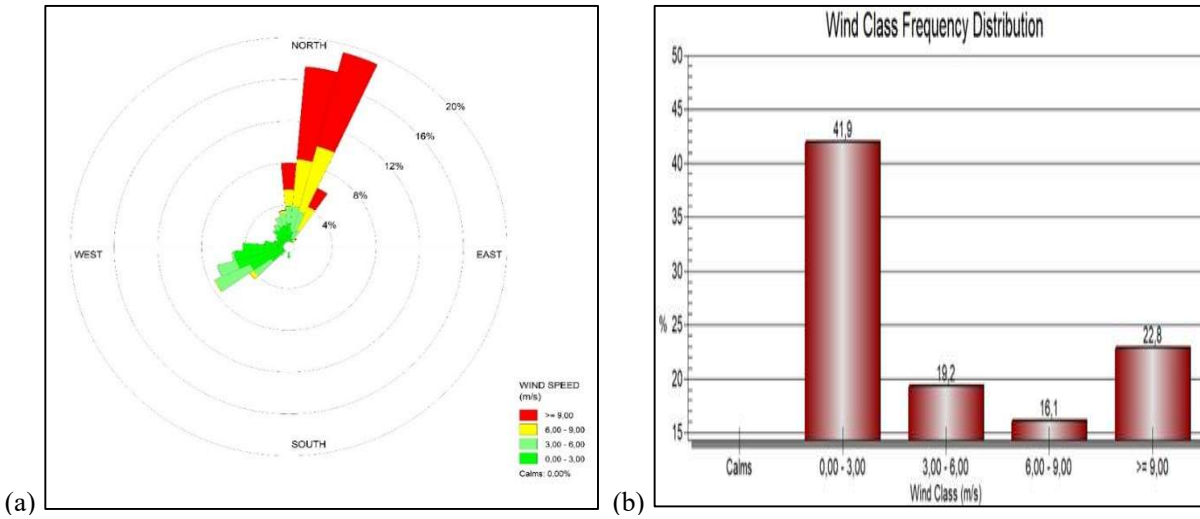


Fig. 4: (a) Wind rose map for 2024. (b) Wind class frequency distribution.

ensuring the simulation reflects the plant's actual operational load during the study period. The complete results of this emission rate calculation are listed in Table 3.

2.3.3. AERMET Processing

AERMET processes hourly meteorological data (in .SAM format) and upper-air data to prepare input files for AERMOD. This processing includes calculating surface parameters (such as albedo, Bowen ratio, and surface roughness) based on land-use characteristics. In this study, the surface parameters were determined based on the site-specific land-use characteristics surrounding PLTU PT.X. The values assigned for the AERMET processing were an Albedo of 0.13, a Bowen Ratio of 0.47, and a Surface Roughness Length of 0.22 m. These parameters, combined with hourly meteorological data and upper-air profiles derived from the Copernicus ERA5 dataset, allow AERMET to internally calculate the atmospheric mixing height and the stability of the air layers. AERMET outputs are surface meteorological files (.SFC) and profile files (.PFL) that are ready for use in AERMOD dispersion modeling. Fig. 5 illustrates the processing steps for AERMET.

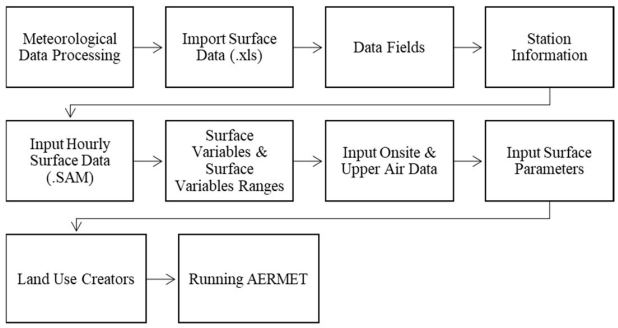


Fig. 5: AERMET processing stages.

2.3.4. AERMOD Processing

Model settings include Control Pathway (defining SO_2 and NO_2 pollutants with an average time of 1 hour), Source Pathway (using stack data and emission rates), Receptor Pathway (Cartesian grid for concentration analysis), and Meteorology Pathway (.SFC and .PFL format files from AERMET). AERMAP is used to integrate topographic data (SRTM3 elevation) into the model grid. Once the data is complete, AERMOD is run for dispersion simulation, producing visualizations of pollutant concentration distributions in the form of maps and isoconcentration lines. Dispersion model processing using AERMOD follows the steps in Fig. 6.

2.3.5. Model Validation Test

The model's performance was evaluated by comparing the SO_2 and NO_2 concentrations from short-term ambient air

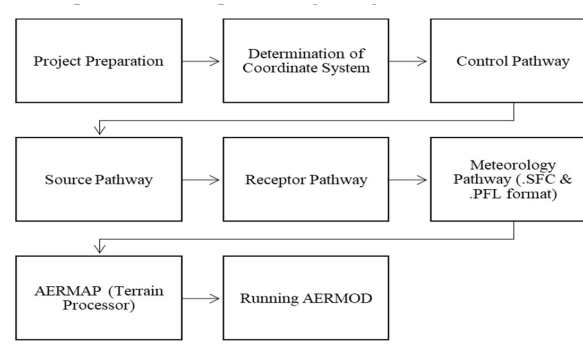


Fig. 6: AERMOD processing stages.

field measurements with the corresponding AERMOD-simulated values. The statistical methods employed for this performance assessment include the calculation of Root Mean Square Error (RMSE), Mean Bias Error (MBE), and Correlation Coefficient (R). These indicators serve to measure the level of agreement between the model's predictions and the observed data during the specific sampling intervals. The RMSE calculation (Hodson 2022) can be performed using Equation 2.

$$RMSE=\sqrt{\frac{1}{n}\sum_{i=1}^{n}(Yi-\hat{Y}i)^2} \quad \ldots(2)$$

where: RMSE – Root Mean Square Error, Yi – actual concentration value, $\hat{Y}i$ – simulated concentration value, n – total number of measurement points.

The Mean Bias Error (MBE) calculation can be performed using Equation 3.

$$MBE=\frac{1}{n}\sum_{i=1}^{n}(\hat{Y}i-Yi) \quad \ldots(3)$$

where: MBE – Mean Bias Error, $\bar{\hat{Y}}i$ – simulated concentration value, Yi – actual concentration value, n – total number of measurement points.

The Correlation Coefficient (R) calculation can be performed using Equation 4.

$$R=\frac{\sum_{i=1}^{n}(\hat{Y}i-\bar{\hat{Y}})(Yi-\bar{})}{\sqrt{\sum_{i=1}^{n}(\hat{Y}i-\bar{\hat{Y}})^2\sum_{i=1}^{n}(Yi-\bar{Y})^2}} \quad \ldots(4)$$

where: R – Correlation Coefficient, $\hat{Y}i$ – simulated concentration value, $\bar{\hat{Y}}i$ – mean of simulated concentrations, Yi – actual concentration value, $\bar{Y}$ – mean of observed concentrations, n – total number of measurement points.

3. RESULTS AND DISCUSSION

3.1. Direct Measurement of SO_2 and NO_2 Concentrations

Fig. 7 shows a graph of direct measurements of SO_2 and NO_2 concentrations during a 1-hour observation period

at two monitoring locations, the PLTU PT.X area and Nii Tanasa Village, based on the intervals of morning, afternoon, evening, and night.

Based on the graph, for SO_2 (Fig. 7(a)), the highest concentrations at both points occurred during the afternoon (PLTU PT.X monitoring point = 39.95 µg m^{-3}; Nii Tanasa Village monitoring point = 28.82 µg m^{-3}). This trend shows that peak operational activity at the coal-fired power plant significantly increases SO_2 emissions during the day. Lower concentrations were observed at the Nii Tanasa Village monitoring point (approximately 700 m away) compared to the monitoring point near PLTU PT.X, mainly due to the distribution and distance from the emission source, as well as the influence of meteorological factors. In addition, this may be due to weather factors such as air humidity, wind direction, and temperature, which affect gas dispersion, resulting in SO_2 concentrations at the Nii Tanasa Village location remaining below the quality standard (Halulanga et al. 2021).

Similar conditions were also observed for NO_2 concentrations (Fig. 7(b)), with the highest value at the PLTU PT.X monitoring point occurring during the afternoon (14.82 µg m^{-3}) due to increased power plant activity. These high concentrations coincided with the highest measured air temperature (34.3 °C) and the lowest humidity (41%), conditions that enhance convective mixing and photochemical activity in the lower atmosphere, thereby facilitating the dispersion and transport of stack emissions. In contrast, at the Nii Tanasa Village monitoring point, the highest concentration was observed in the morning at 12 µg m^{-3}. This suggests that the difference in concentration between the two monitoring points confirms the strong influence of distance from the emission source, although local factors such as morning traffic may also contribute. However, the highest concentrations measured during 1 hour for SO_2 (39.95 µg m^{-3}) and NO_2 (14.82 µg m^{-3}) at both monitoring locations were still below the ambient air quality standards for 1 hour set by Government Regulation Number 22 of 2021 (SO_2 limit: 150 µg m^{-3}; NO_2 limit: 200 µg m^{-3}).

3.2. AERMOD SO_2 and NO_2 Concentrations

3.2.1. SO_2 Concentration

Table 4 presents the AERMOD one-hour SO_2 concentrations across four time intervals synchronized with the direct measurement periods, showing that the overall highest concentrations occurred at the PLTU PT.X monitoring point, with a peak value of 31.87 µg m^{-3} recorded at night. The high concentration at this point correlates with its closer proximity to the primary emission source compared to Nii Tanasa Village. Furthermore, based on the wind rose (Fig. 4), although dominant wind directions vary, SO_2 is a local pollutant whose concentrations tend to be highest at locations nearest to the emission source. The phenomenon of increased nighttime concentrations, particularly at the PLTU PT.X monitoring point, indicates the influence of stable atmospheric conditions. Atmospheric stability is significantly higher at night than during the day (Kusumawati 2025). Variations in atmospheric stability levels can occur based on the intensity of temperature differences between the air mass and the surrounding air (Sasmita et al. 2021). The cooling air at the PLTU PT.X monitoring point during the night is further evidenced by monitoring data, which showed a temperature of 26.5°C and high humidity of 76.7%. Conversely, in Nii Tanasa Village, the peak concentration of 10.81 µg m^{-3} occurred in the morning. This is likely due to the prevailing stable temperature and humidity conditions; at 29.9°C and 62.3% humidity, the SO_2 concentrations modeled by AERMOD remained insufficiently dispersed into the higher atmospheric layers. Stable atmospheric conditions in the morning restrict vertical air movement, causing pollutants to be trapped near the ground surface

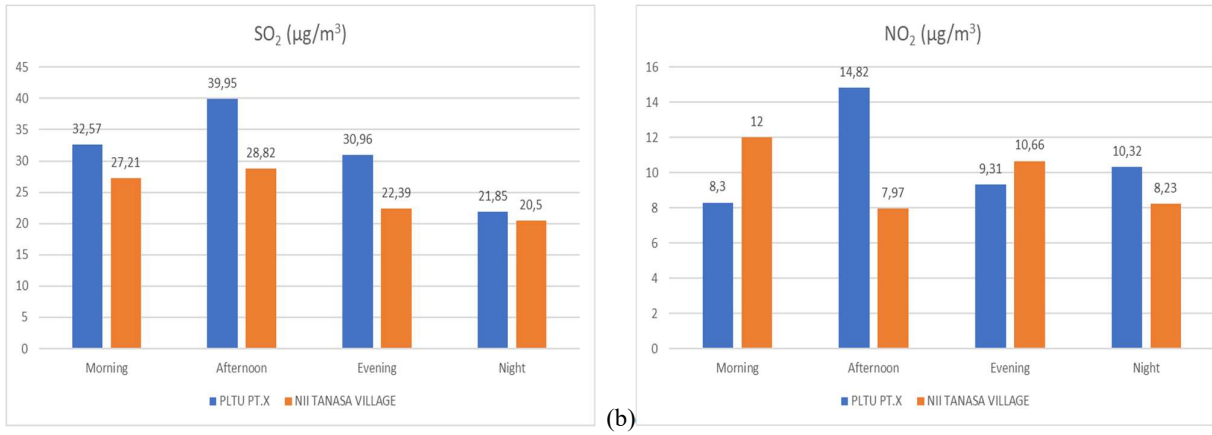


Fig. 7: (a) SO_2 direct measurement. (b) NO_2 direct measurement.

(the accumulation phase) before rising daytime temperatures trigger vertical dilution.

3.2.2. NO_2 Concentration

Table 5 presents the AERMOD one-hour NO_2 concentrations across four time intervals (morning, afternoon, evening, and night) synchronized with the direct measurement periods. At the PLTU PT.X monitoring point, the highest NO_2 concentration occurred at night, reaching 10.56 µg m^{-3}, which is higher than the concentrations recorded during the morning, afternoon, and evening at the same location. A similar pattern of significant nighttime increase was observed in Nii Tanasa Village, with a concentration of 4.45 µg m^{-3}. The increase in NO_2 concentrations at night in these two locations also indicates stable atmospheric conditions, such as temperature inversions, which trap air movement. Similar to SO_2 concentrations, the meteorological inputs used by AERMOD indicate more stable nighttime temperature and humidity conditions. This inhibits vertical air movement and affects pollutants near the ground surface, leading to increased pollution at the human respiratory level (Srisantyorini 2025).

3.3. AERMOD Dispersion Modeling

3.3.1. Dispersion of SO_2

For 1-hour and 24-hour averaging periods based on the full annual meteorology of 2024, Fig. 8(a) and (b) show that the modeled annual maximum concentrations for the highest average 1-hour SO_2 concentrations at the monitoring points of PLTU PT.X and Nii Tanasa Village were 33.86 µg m^{-3} and 29.05 µg m^{-3}, respectively. At the same time, the modeled annual maximum 24-hour averages were 10.65 µg m^{-3} and 7.42 µg m^{-3}, respectively. Meanwhile, Fig. 8(c), (d), (e), and (f) illustrate the relationship between concentration and distance during that period based on the prevailing wind direction. Note that these annual modeled maxima naturally differ from the specific hourly values reported in Tables 4 and 5, which correspond strictly to the synchronized field-sampling intervals on October 21, 2024.

The SO_2 distribution pattern during the 2024 period predominantly points north-northeast toward the sea, following the prevailing wind direction. At the PLTU PT.X monitoring point (±7.5 m from the stack base), Fig. 8(c) shows initial predicted concentrations of approximately 34.02 µg m^{-3}. However, it should be noted that for a 45-m stack, receptors located within this immediate near-field zone (1–7.5 m) fall below the typical plume trajectory. While the model accounts for building downwash effects where aerodynamic turbulence can influence dispersion, the physical meaningfulness of predictions at such proximity is limited, as the plume has not yet fully reached ground level.

Table 4: AERMOD SO_2 concentration.

Monitoring Point	Coordinate Point		Time	SO_2 Concentration (µg m^{-3})
	UTM X	UTM Y		
PLTU PT.X	448623.28	9569522.39	Morning	30.92
			Afternoon	22.84
			Evening	20.23
			Night	31.87
Nii Tanasa Village	448364.13	9568947.04	Morning	10.81
			Afternoon	8.41
			Evening	8.41
			Night	7.23

Table 5: AERMOD NO_2 concentration.

Monitoring Point	Coordinate Point		Time	NO_2 Concentration (µg m^{-3})
	UTM X	UTM Y		
PLTU PT.X	448623.28	9569522.39	Morning	7.87
			Afternoon	7.37
			Evening	7.37
			Night	10.56
Nii Tanasa Village	448364.13	9568947.04	Morning	3.33
			Afternoon	3.06
			Evening	3.06
			Night	4.45

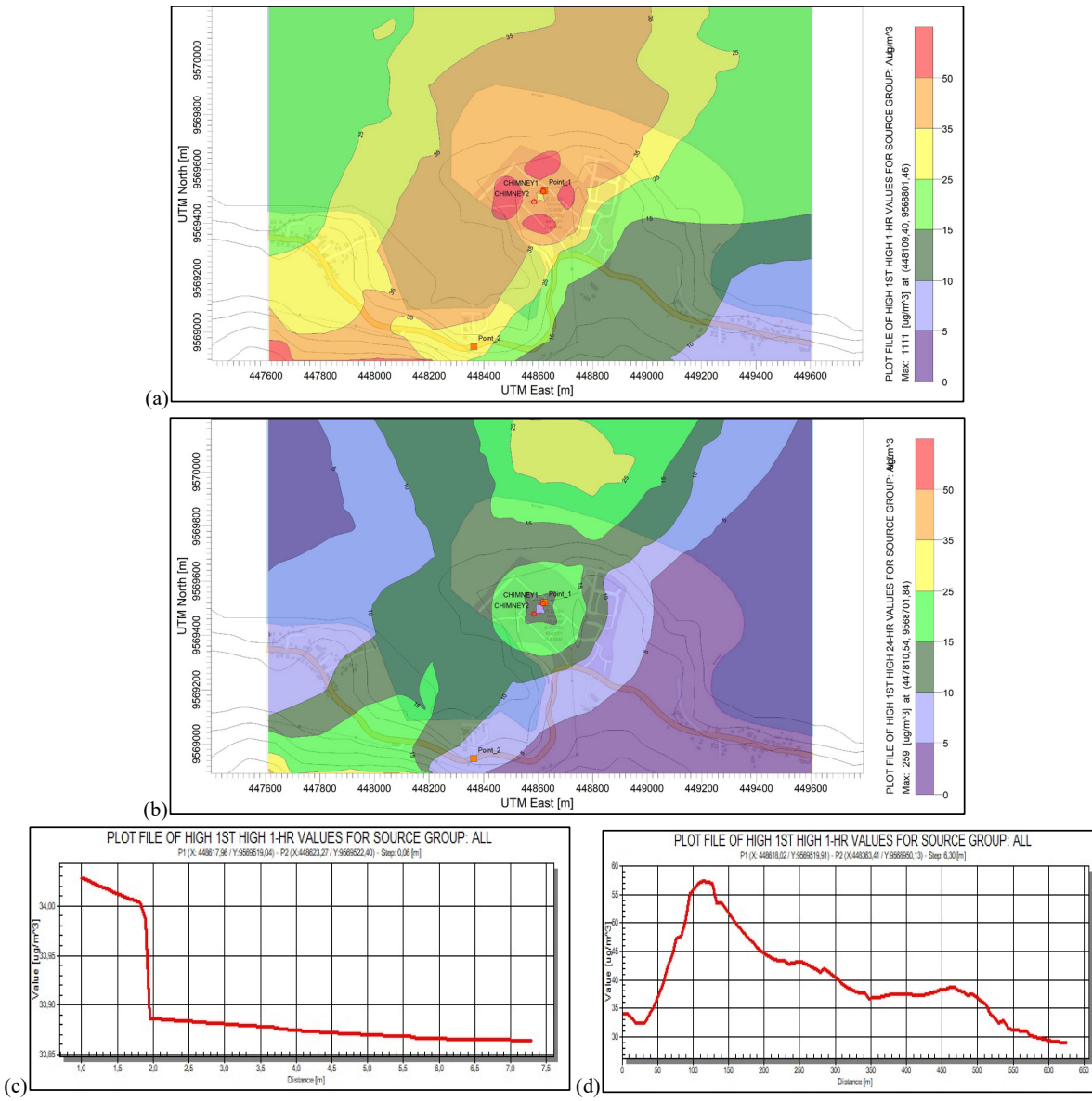


Fig. 8: (a) 1-hour SO_2 dispersion. (b) 24-hour SO_2 dispersion. (c) SO_2 at point 1 (PLTU PT.X) for 1 hour. (d) SO_2 at point 2 (Nii Tanasa Village) for 1 hour. (e) SO_2 at point 1 (PLTU PT.X) for 24 hours. (f) SO_2 at point 2 (Nii Tanasa Village) for 24 hours.

In contrast, a more dynamic and physically representative pattern is observed towards Nii Tanasa Village (Fig. 8(d)). This area shows a classic dispersion profile where the concentration reached a significant peak of approximately 57 μg m⁻³ at a distance of 110–120 m from the source, representing the primary plume touchdown point. After this peak, the concentration gradually decreased and stabilized, reaching 29.05 μg m⁻³ at the monitoring point in Nii Tanasa Village (±650 m). For the 24-hour average (Fig. 8(e) and 8(f)), the maximum concentrations at the PLTU PT.X and Nii Tanasa Village receptors were 10.65 μg m⁻³ and 7.42 μg m⁻³, respectively. All predicted values remained well below the ambient air quality standards (150 μg m⁻³ for 1-hour and 75 μg m⁻³ for 24-hour). These findings are consistent with previous observations that concentration patterns are heavily influenced by dominant wind directions and distance-dependent dispersion factors (Sarwono et al. 2022).

3.3.2. Dispersion of NO_2

As with SO_2, Fig. 9(a) and (b) show the maximum NO_2 concentrations for the 1-hour averaging period at the PLTU PT.X and Nii Tanasa Village monitoring points, which were 12.94 μg m⁻³ and 11.10 μg m⁻³, respectively. At the same

time, the highest 24-hour averages were 4.07 µg m^{-3} and 2.83 µg m^{-3}. Meanwhile, Fig. 9(c), (d), (e), and (f) illustrate the relationship between concentration and distance during that period based on the prevailing wind direction.

The NO_2 dispersion pattern during the 2024 period follows a similar trend to SO_2, predominantly spreading north-northeast from the PLTU PT.X chimney toward the sea, reflecting the influence of the prevailing wind direction. Fig. 9(c) illustrates the NO_2 concentration within the immediate near-field zone (up to 7.5 m) from the stack base. While the model calculates an elevated concentration of 12.94 µg m^{-3} at this point, it is acknowledged that for a 45-m stack, receptors at this distance are situated below the primary plume trajectory. These near-field values should be interpreted with caution, as they may reflect the model's mathematical treatment of aerodynamic turbulence (building downwash) rather than a physically representative grounding of the plume so close to the source. Meanwhile, for the 24-hour average (Fig. 9(e)), the dispersion follows a smaller scale with a maximum concentration of 4.07 µg m^{-3} at the same receptor.

In contrast, the dispersion toward Nii Tanasa Village (Fig. 9(d)) shows a more physically representative and

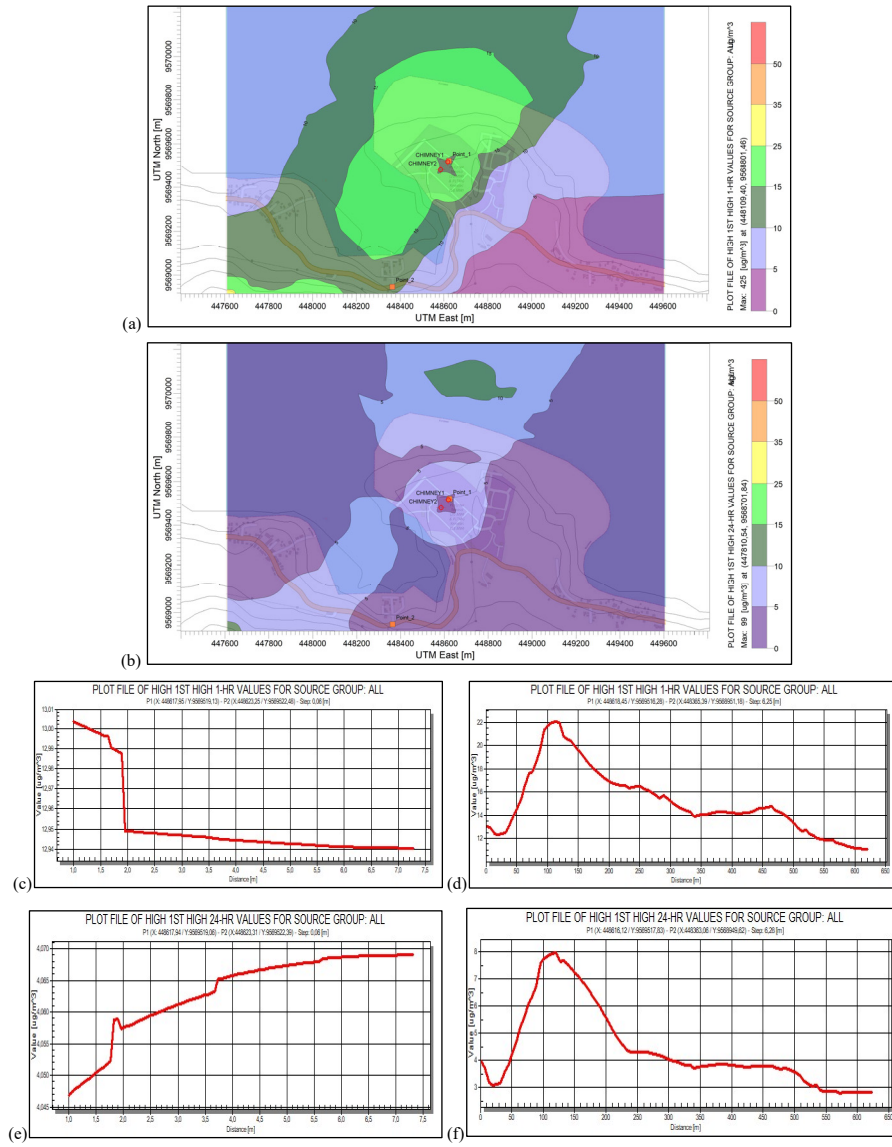


Fig. 9: (a) 1-hour NO_2 dispersion. (b) 24-hour NO_2 dispersion. (c) NO_2 at point 1 (PLTU PT.X) for 1 hour. (d) NO_2 at point 2 (Nii Tanasa Village) for 1 hour. (e) NO_2 at point 1 (PLTU PT.X) for 24 hours. (f) NO_2 at point 2 (Nii Tanasa Village) for 24 hours.

classic dispersion pattern. The concentration exhibits an upward trend, peaking at approximately 22 μg m^{-3} at a distance of 100 m from the source. This peak represents the plume touchdown point, occurring after the plume undergoes thermal buoyancy (plume rise) and reaches the ground level due to wind transport, before gradually decreasing to 11.10 μg m^{-3} at the ±650 m receptor. A similar trend is observed for the 24-hour average (Fig. 9(f)), which peaks at 8 μg m^{-3} within the 100–150 m range before declining to 2.83 μg m^{-3} at the monitoring point. Despite these fluctuations, all NO_2 concentration values remained well below the national ambient air quality standards (200 μg m^{-3} for 1-hour and 65 μg m^{-3} for 24-hour).

3.4. Model Validation Test (RMSE, MBE, and R)

Table 6 presents a comparison between the SO_2 and NO_2 concentrations obtained from direct measurements and the AERMOD model predictions at two monitoring points: the PLTU PT.X and Nii Tanasa Village. To ensure a valid comparison, the AERMOD model output selected for this analysis was synchronized with the exact date and hourly intervals (morning, afternoon, evening, and night) of the field sampling conducted on October 21, 2024. While this temporal alignment allows for a snapshot performance check, it is acknowledged that a single day of data is insufficient to fully represent the model's annual simulation. Direct monitoring results show that SO_2 concentrations near the PLTU PT.X ranged from 21.85 μg m^{-3} to 39.95 μg m^{-3}, while AERMOD estimated 20.23 μg m^{-3} to 31.87 μg m^{-3}. These discrepancies are primarily due to the receptor's close proximity to the emission source (±7.5 m). For a 45-m stack, this distance falls outside the physically meaningful predictive zone of AERMOD, as the exhaust gas is still in the buoyancy (plume rise) phase and has not yet grounded. Consequently, the higher field measurements at this location likely capture low-level fugitive emissions or local background sources within the plant area that are not accounted for in the stack-only model. A similar pattern was observed for NO_2, where field measurements ranged from 8.3 μg m^{-3} to 14.82 μg m^{-3}, while the AERMOD simulation estimated lower concentrations between 7.37 μg m^{-3} and 10.56 μg m^{-3} due to the same near-field modeling limitations.

Meanwhile, at the Nii Tanasa Village monitoring point (±650 m), the AERMOD model showed a better alignment with the dispersion physics, although simulated values were still lower than direct measurements. For SO_2, field measurements ranged from 20.5 μg m^{-3} to 28.82 μg m^{-3}, whereas AERMOD estimated 7.23 μg m^{-3} to 10.81 μg m^{-3}. Similarly, for NO_2, field measurements ranged from 8.23 μg m^{-3} to 12 μg m^{-3}, while AERMOD modeling results ranged from 3.06 μg m^{-3} to 4.45 μg m^{-3}. These results indicate that AERMOD is more representative at greater distances where the plume has undergone diffusion and wind transport. Discrepancies may arise because field monitoring captures cumulative impacts from various sources, such as traffic and community activities, while the model focuses strictly on boiler stack emissions (Ramadhani 2017). Therefore, given the inherent modeling uncertainties and the limited sampling

Table 6: Comparison of direct measurements with the AERMOD model.

Monitoring Point	Parameters	Time	Direct Measurement	AERMOD
PLTU PT.X	SO_2 (μg m^{-3})	Morning	32.57	30.92
		Afternoon	39.95	22.84
		Evening	30.96	20.23
		Night	21.85	31.87
	NO_2 (μg m^{-3})	Morning	8.3	7.87
		Afternoon	14.82	7.37
		Evening	9.31	7.37
		Night	10.32	10.56
Nii Tanasa Village	SO_2 (μg m^{-3})	Morning	27.21	10.81
		Afternoon	28.82	8.41
		Evening	22.39	8.41
		Night	20.5	7.23
	NO_2 (μg m^{-3})	Morning	12	3.33
		Afternoon	7.97	3.06
		Evening	10.66	3.06
		Night	8.23	4.45

duration, these results should be interpreted as a preliminary screening-level assessment.

To evaluate the performance of the AERMOD model in predicting the concentrations of SO_2 and NO_2, statistical performance was assessed by comparing the model results with direct field measurements. Table 7 presents the results of the Root Mean Square Error (RMSE) calculated based on Equation 2, Mean Bias Error (MBE) calculated based on Equation 3, and Correlation Coefficient (R) calculated based on Equation 4 using eight paired data points for each pollutant.

The validation results show that the RMSE values for SO_2 and NO_2 are 14.00 μg m^{-3} and 5.37 μg m^{-3}, respectively. While these values reflect the absolute error magnitude of the residuals, they represent a noticeable deviation relative to the observed field mean concentrations. Theoretically, a smaller RMSE (approaching 0) signifies a better fit between modeled and measured data (Hamdanah & Fitrianah 2021). In this study, the calculated RMSE values serve as a baseline measure of absolute deviation during the sampled periods, highlighting the variance associated with short-term screening assessments rather than confirming precise model fit.

The Mean Bias Error (MBE) was employed to assess the systematic bias of the forecasting model by measuring the average difference between the predicted and actual values (Kato 2016). The calculation yielded negative MBE values for both pollutants: -10.44 μg m^{-3} for SO_2 and -4.32 μg m^{-3} for NO_2. A negative MBE indicates that the forecasted values are, on average, smaller than the actual values, signifying a systematic underprediction (Kato 2016). In the context of this study, this trend is commonly observed in dispersion modeling when the simulation focuses primarily on specific point sources, such as the power plant stack, while actual field measurements capture the cumulative impact of additional background concentrations from other local activities or non-modeled sources. Consequently, this negative bias highlights the inherent limitation of point-source modeling in capturing total ambient levels, underscoring that the predicted concentrations reflect only the specific contribution of the stack emissions rather than total cumulative field conditions.

Regarding the Correlation Coefficient (R), the model yielded values of 0.36 for SO_2 and 0.12 for NO_2. The correlation coefficient quantifies the strength and direction of the linear relationship between two variables, where a score close to 1.0 indicates strong correlation and a value close to 0 indicates a negligible relationship (Thieu et al. 2023). These results reflect a weak linear association for SO_2 and a negligible correlation for NO_2, confirming that the model struggles to capture precise hourly temporal fluctuations during the sampling period. Such low correlation values are anticipated when evaluating a small sample size (n = 8) over a short sampling window against a simulation driven by a full-year meteorological dataset. Consequently, while the model remains informative for characterizing general spatial dispersion trends around PLTU PT.X and Nii Tanasa Village as a screening-level assessment, its temporal predictive capability for exact hourly variations is limited.

Table 7: RMSE, MBE, and R test results.

Parameters	RMSE	MBE	R
SO_2 (μg m^{-3})	14	-10.44	0.36
NO_2 (μg m^{-3})	5.37	-4.32	0.12

4. CONCLUSIONS

This study concludes that while direct measurements and AERMOD simulations exhibit differing diurnal peak intervals (daytime and nighttime, respectively), all resulting concentrations consistently remain below national ambient air quality standards. Spatially, the dispersion follows a north-northeast trajectory, with modeled concentrations initially increasing to a plume touchdown peak at approximately 100–120 m downwind before gradually declining with distance. This spatial profile reflects typical high-stack dispersion behavior, acknowledging that the immediate near-field receptor (~7.5 m) captures lower concentrations prior to full plume touchdown. Although temporal discrepancies exist between observed and modeled peaks, AERMOD provides a useful screening-level evaluation for characterizing the overall spatial dispersion pattern around PLTU PT.X and Nii Tanasa Village.

Evaluation of statistical metrics including RMSE (14.00 μg m^{-3} for SO_2 and 5.37 μg m^{-3} for NO_2), negative MBE values, and low correlation coefficients (R) highlights the inherent statistical limitations in predicting exact short-term temporal variations, thereby reinforcing the application of the model primarily for screening-level spatial assessments rather than precise temporal forecasting. While current findings confirm that ambient concentrations remain within regulatory limits, they clearly emphasize the limitations of single-day sampling and underscore the necessity of continuous monitoring and multi-season sampling to capture long-term variability. These insights provide an initial baseline for guiding future air quality management and environmental policy planning in the industrial area.

5. ACKNOWLEDGMENTS

The authors would like to thank PLTU PT.X in Lalonggasumeeto District, Konawe Regency, Southeast

Sulawesi, Indonesia, for granting the authors access and permission to conduct research at the location.

6. REFERENCES

Alchamdani, 2019. Exposure of NO_2 and SO_2 to health risks of public fuel station (SPBU) workers in Kendari City. *Jurnal Kesehatan Lingkungan*, 11(4), pp.319–330. [DOI]

Alviani, M., Anggraini, F.J. and Rodhiyah, Z., 2022. Pemodelan PM2,5 pada musim kemarau menggunakan software Graz Largangian Model di Kecamatan Kota Baru Kota Jambi. *Jurnal Teknik Lingkungan UM Kendari*, 2(2), pp.5–9. [DOI]

Barata, L.O.A., 2024. Sistem perawatan water treatment plant (WTP) PLTU Nii Tanasa 3 × 10 MW. *Piston Jurnal Teknologi*, 9(1), pp.24–35. [DOI]

Government Regulation of the Republic of Indonesia Number 22 of 2021. Implementation of environmental protection and management (in Indonesian). Jakarta. Available at: https://jdih.kehutanan.go.id/new2/home/open_indonesia_file/PP_22_TAHUN_2021_PENYELENGGARAAN_LH_c_menlhk_02222021144819.pdf

Halulanga, A.J., Rosdiana, R. and Adami, A., 2021. Uji kandungan gas sulfur dioksida (SO_2) pada udara ambien akibat adanya pembakaran batubara PLTU Nii Tanasa, Sulawesi Tenggara. *Jurnal Teknik Lingkungan UM Kendari*, 1(2), pp.5–10. [DOI]

Hamdanah, F.H. and Fitrianah, D., 2021. Analisis performansi algoritma linear regression dengan generalized linear model untuk prediksi penjualan pada usaha mikra, kecil, dan menengah. *Jurnal Nasional Pendidikan Teknik Informatika*, 10(1), pp.23–32. [DOI]

Hodson, T.O., 2022. Root-mean-square error (RMSE) or mean absolute error (MAE): When to use them or not. *Geoscientific Model Development*, 15(14), pp.5481–5487. [DOI]

Junarto, G.E., 2021. Penerapan model AERMOD untuk dispersi emisi gas buangan PLTU dan analisis risiko kesehatan lingkungan (studi: PLTU Tonasa, Kec. Bungoro, Kabupaten Pangkep). Master's thesis, Hasanuddin University, Makassar. Available at: https://repository.unhas.ac.id/id/eprint/15398/2/P032171203_tesis_bab%201-2.pdf

Kato, T., 2016. Prediction of photovoltaic power generation output and network operation. In: *Integration of Distributed Energy Resources in Power Systems*, pp.77–108. [DOI]

Kusumawati, R.D., 2025. Analisis dispersi nitrogen dioksida (NO_2) udara ambien di Kawasan Budaya, Kota Yogyakarta menggunakan pemodelan AERMOD. Skripsi, Universitas Islam Indonesia, Yogyakarta. Available at: https://dspace.uii.ac.id/bitstream/handle/123456789/56033/21513157.pdf?sequence=1&isAllowed=y

Munawaroh, N., Syamsyiatun, S. and Fikri, A.A., 2019. Sistem pengolahan air dan pengendalian limbah di PLTU Tanjung Jati-B Desa Tubanan Kembang Jepara. *Jurnal Bakti Saintek: Jurnal Pengabdian Masyarakat Bidang Sains dan Teknologi*, 3(2), pp.73–76. [DOI]

Ningsih, S., 2020. Model sebaran SO_2 dan NO_x PLTU Jeneponto PT. Bosowa Energi. *Jurnal AKRAB Juara*, 5(2), pp.231–238. Available at: https://www.akrabjuara.com/index.php/akrabjuara/article/view/1079/954

Nugraha, P.S., Setiawan, A. and Yustian, I., 2023. AERMOD modeling analysis of CO and NO_x parameters from diesel generator emission sources in the coal mining industry. *Sriwijaya Journal of Environment*, 8(2), pp.92–97. [DOI]

Oktaviani, S., Siregar, S.H., Fauzi, R., Reflis and Utama, S.P., 2023. Gangguan ekosistem laut sebagai dampak keberadaan PLTU Teluk Sepang Bengkulu: Sebuah telaah pustaka. *INSOLOGI: Jurnal Sains dan Teknologi*, 2(6), pp.1061–1068. [DOI]

Putra, D.Y.P. and Nisa, S.Q.Z., 2023. Uji model AERMOD terhadap emisi di PT. X Jawa Timur. *ESEC Proceeding Environmental Science and Engineering Conference*, 4(1), pp.370–379. Available at: https://esec.upnvjt.com/index.php/prosiding/article/download/256/182

Rahmadina, I., 2022. Dampak operasional PLTU terhadap kesehatan masyarakat di Desa Tanjung Tiram Kecamatan Moramo Utara Kabupaten Konawe Selatan. Skripsi, Halu Oleo University, Kendari.

Ramadhani, I.S., 2017. Pemantauan kualitas udara ambien dan pemodelan Gauss dispersion gas nitrogen dioksida (NO_2) dari emisi industri kayu lapis di Dusun Kalimati, Tirtomartani, Kalasan, Sleman, D.I. Yogyakarta. Skripsi, Universitas Islam Indonesia, Yogyakarta. Available at: https://dspace.uii.ac.id/handle/123456789/33142

Salari, M., Abdolmaleki, M.J., Shahid, E.S. and Akhoundi, B., 2026. Dispersion of particulate matter using AERMOD model and health risk assessment: Case study Saveh gypsum industry. *Iranica Journal of Energy and Environment*, 17(2), pp.372–381. [DOI]

Sarwono, E., Wijayanto, E., Huda, H., Harrits, R.F. and Zain, I.F., 2022. Dispersi SO_2 dan NO_2 dari cerobong auxiliary boiler industri methanol PT KMI menggunakan Gaussian plume model AERMOD di Kota Bontang, Kalimantan Timur, Indonesia. *Jurnal Chemurgy*, 6(2), pp.109–117. Available at: http://e-journals.unmul.ac.id/index.php/TK

Sasmita, A., Andrio, D. and Nopita, R., 2021. Dispersi SO_2 dan NO_2 dari pembangkit listrik tenaga uap Tembilahan, Riau. *Jurnal Ilmiah Teknik Lingkungan*, 13(2), pp.98–107. [DOI]

Srisantyorini, T., 2025. *Analisis Kualitas Udara Dampak terhadap Lingkungan dan Kesehatan*. 1st ed. Mafy Media Literasi Indonesia, Solok, Indonesia. Available at: https://penerbitmafy.com/wp-content/uploads/2025/12/ANALISIS-KUALITAS-UDARA-Dampak-Terhadap-Lingkungan-dan-Kesehatan.pdf

Tampa, G.M., Maddusa, S.S. and Pinontoan, O.R., 2020. Analisis kadar sulfur dioksida (SO_2) udara di Terminal Malalayang, Kota Manado tahun 2019. *Indonesian Journal of Public Health and Community Medicine*, 1(3), pp.87–92. [DOI]

Thieu, N.V., Barma, S.D., Lam, T.V., Kisi, O. and Mahesha, A., 2023. Groundwater level modeling using augmented artificial ecosystem optimization. *Journal of Hydrology*, 617, p.129034. [DOI]

Tran, Q.A., Nguyen, N.H.T., Nguyen, P.Q. and Nguyen, A.M., 2022. Simulation of thermal power plant source contribution to ambient air concentration in Cam Pha City, Quang Ninh Province using AERMOD dispersion model. *Journal of Mining and Earth Sciences*, 63(3), pp.35–42. [DOI]

United States Environmental Protection Agency (US EPA), 2024. *Recommended Procedures for Development of Emissions Factors and Use of the WebFIRE Database*. Retrieved May 19, 2025, from: https://www.epa.gov/system/files/documents/2024-09/final-webfire-procedures-document_aug-2024.pdf

Wangsa, D., Bachtiar, V.S. and Raharjo, S., 2022. Uji model AERMOD terhadap sebaran particulate matter 10 µm (PM_{10}) di sekitar kawasan PT Semen Padang. *Jurnal Ilmu Lingkungan*, 20(2), pp.291–301. [DOI]

Zakaria, R., Aly, S.H. and Annisa, 2020. Air dispersion modeling of gas turbine power plant emissions in Makassar by using AERMOD. *IOP Conference Series: Earth and Environmental Science*, 419, p.012153. [DOI]